Jesty, J., & Nemerson, Y. (1976) *Methods Enzymol. 45*, 95.
Klotz, I. M. (1982) *Science (Washington, D.C.) 217*, 1247.
Laemmli, U. K. (1970) *Nature (London) 227*, 680.
Mendel, C. M., Licko, M., & Kane, J. R. (1985) *J. Biol. Chem. 260*, 3451.
Mimms, L. T., Zampighi, G., Nozaki, Y., Tanford, C., & Reynolds, J. A. (1981) *Biochemistry 20*, 833.
Nelsestuen, G. L., Kisiel, W., & Di Scipio, R. G. (1978) *Biochemistry 17*, 2134.
Nemerson, Y. (1968) *J. Clin. Invest. 47*, 72.
Pitlick, F. A., & Nemerson, Y. (1970) *Biochemistry 9*, 5105.
Radcliffe, R., & Nemerson, Y. (1975) *J. Biol. Chem. 250*, 388.
Reynolds, J. A., Nozaki, Y., & Tanford, C. (1983) *Anal. Biochem. 130*, 471.
Rothman, J. E., & Lenard, J. (1977) *Science (Washington, D.C.) 195*, 743.
Silverberg, S. A., Nemerson, Y., & Zur, M. (1977) *J. Biol. Chem. 252*, 8481.
Van Lenten, L., & Ashwell, G. (1971) *J. Biol. Chem. 246*, 1889.
Zur, M., & Nemerson, Y. (1981) *Methods Enzymol. 80*, 237.
Zur, M., Radcliffe, R. D., Oberdick, J., & Nemerson, Y. (1982) *J. Biol. Chem. 257*, 5623.
Zwaal, R. F. A., Comfurius, P., & van Deenen, L. L. M. (1977) *Nature (London) 268*, 358.

An Ordered Addition, Essential Activation Model of the Tissue Factor Pathway of Coagulation: Evidence for a Conformational Cage†

Yale Nemerson*

Division of Thrombosis Research, Department of Medicine, Mt. Sinai School of Medicine of The City University of New York, New York, New York 10029

Rodney Gentry

Department of Mathematics and Statistics, University of Guelph, Guelph, Ontario, Canada N1G 2W1

Received May 30, 1985; Revised Manuscript Received January 24, 1986

ABSTRACT: One way in which coagulation may be initiated is by the action of factor VIIa (a plasma serine protease) and tissue factor (a membrane-bound lipid-dependent glycoprotein). We show that in the absence of either factor VIIa or tissue factor, the activation of the natural coagulation substrates, factors IX and X, is not detectable; i.e., tissue factor is an essential activator. We propose that the reaction is fully ordered; that is, the enzyme–activator complex picks up substrate to form a ternary product forming species. Our model precludes the formation of enzyme–substrate and activator–substrate complexes. We have derived equations for the two possible variations of this model: one in which product formation is accompanied by the release of the enzyme–activator complex and the other in which product, free enzyme, and free activator are formed with each catalytic cycle. Our data support only the former which is consistent with both steady-state and rapid equilibrium assumptions. The model is supported by experiments using a monoclonal anti-tissue factor antibody, which affects only the $K_{m\,app}$, and a modified form of factor VIIa, which, depending on the sequence in which reagents are added to the reaction, either decreases the V_{max} or increases the $K_{m\,app}$. We present equations describing the initial velocity of these reactions. Utilizing dilution–jump experiments, we show that the system is hysteretic and suggest that this phenomenon is due to a slow release of enzyme from activator. However, the kinetically determined dissociation constant of enzyme and activator, previously found to be 4.5 nM under equilibrium conditions, was estimated to be 0.04–0.09 nM. Accordingly, we examined other essential activation models in which the product-forming species consists of a complex of enzyme, activator, and substrate at a molar ratio of 1:1:1; none could account for the apparent tight binding of enzyme and activator. We therefore postulate an ordered addition, essential activation model in which the enzyme undergoes two conformational transformations: one as a consequence of binding to tissue factor, resulting in a species which binds to and hydrolyzes its natural substrates. The other conformational change in the enzyme is induced by substrate, resulting in a species which binds more tightly to its activator. Thus, we hypothesize a "conformational cage" which precludes the dissociation of enzyme from activator while significant concentrations of substrate are present.

We have previously presented evidence that two catalytically active proteins, factor VII (a zymogen) and its two-chain derivative factor VIIa, participate in the initiation of the tissue factor pathway of coagulation (Zur et al., 1982). We also found that both forms of factor VII exhibit a dependence on tissue factor, a membrane-bound glycoprotein: in the absence of tissue factor, no product formation is observed. With respect to coagulant activity, then, tissue factor is an obligatory or "essential" activator.

When factor VII or factor VIIa is reacted with diisopropyl fluorophosphate (DFP),[1] all coagulant activity is lost. Each

† Supported, in part, by Grant HL 29019 from the National Institutes of Health and Grant A9100 from NSERC, Canada.

0006-2960/86/0425-4020$01.50/0

derivatized protein, however, markedly inhibits a tissue factor dependent coagulation reaction (Zur et al., 1982). We interpreted the inhibition as arising from the formation of catalytically inert complexes between tissue factor and the modified protein, thus reducing the available activator concentration. Our data, then, suggest that tissue factor is an essential activator and that the central product-forming species in these reactions is a complex of the activator (A), the enzyme (E) (either factor VII or factor VIIa), and the substrate (S) (either factor IX or factor X).

The central AES complex could arise from the ordered addition of reactants or by the random assembly of the species. In a random model, enzyme, for example, could form ES and AE complexes to which activator or substrate, respectively, would add to form the central complex. In this paper, we present evidence that the only complexes which do exist are AE and AES; that is, the reaction is fully ordered:

$$E + A \overset{K_1}{\leftrightarrow} AE + S \overset{K_2}{\leftrightarrow} AES \xrightarrow{k_{cat}} P \qquad (I)$$

where K_1 and K_2 are equilibrium dissociation constants and k_{cat} is the catalytic rate constant.

In earlier experiments, the derivatized proteins, diisopropylphosphoro-factor VII (DIP-factor VII) and DIP-factor VIIa, were found to inhibit factor IX activation by decreasing the V_{max} without affecting the $K_{m\,app}$ (Zur et al., 1982). These experiments were performed by assembling all the reactants and then initiating the reaction with Ca^{2+}, an obligatory ion. In this paper, we show that a different "antiactivator", a monoclonal antibody directed toward the factor VII binding site on tissue factor (Carson et al., 1985), behaves differently: in a similar experiment, the $K_{m\,app}$ rose whereas the V_{max} remained unchanged. We have explored these effects and apparent contradictions and show that the sequence in which reagents are added to the reaction mixture determines the apparent mode of inhibition engendered by the DIP proteins. We interpret this result as arising from a dissociation of enzyme from activator which is slow relative to the formation of AES from AE and S. This concept was further explored by examining reaction velocities measured after enzyme, activator, and calcium ions were preincubated at high concentration and added to the reaction following a "dilution–jump". The observed velocities considerably exceeded those obtained in control experiments, indicating a slow dissociation of enzyme from activator.

However, when comparing the equilibrium dissociation constant of the AE complex determined kinetically with that obtained under equilibrium conditions, we find a large discrepancy, the latter being some 50–100-fold greater than the former. To investigate this anomaly, we have derived kinetic equations for each of the possible ways enzyme, activator, and substrate can combine with a stoichiometry of 1:1:1 to form the productive AES complex. We conclude that only an ordered addition model fits our data. We therefore extend model I to accommodate the apparent tight binding of enzyme to activator. The model we propose involves reciprocal interactions in the ternary complex in which tissue factor binds to factor VIIa, thus enabling the enzyme to recognize and hydrolyze its natural substrate, factor X; upon binding to the substrate, we hypothesize that the enzyme is transiently altered such that it binds more tightly to the activator.

Materials and Methods

The murine monoclonal antibody to bovine brain tissue factor was prepared and characterized by S. Carson (presently at the University of Colorado) and R. Bach of our group (Carson et al., 1985).

Essentially homogeneous preparations of bovine factors VII, IX, and X were prepared and quantified as previously described (Bach et al., 1984; Kalousek et al., 1975; Jesty & Nemerson, 1976). Factor VIIa was prepared by cleaving factor VII with factor Xa as previously described (Radcliffe & Nemerson, 1975). The resultant product was in the two-chain form as judged by electrophoresis of a reduced sample (Laemmli, 1970). The enzyme possessed 100–120 times the coagulant activity of the zymogen (Bach et al., 1984).

Tissue factor, a membrane-bound glycoprotein, is delipidated during purification, in which state it is inactive. The apoprotein, which was purified as previously described (Bach et al., 1981), was reactivated by incorporation into vesicles consisting of phosphatidylcholine (egg) and phosphatidylserine (bovine) at the indicated ratios. Unless stated, relipidation was accomplished with pure phosphatidylcholine. The lipids were obtained from Supelco, Inc., Bellefonte, PA. Reconstitution was accomplished by using the octyl glucoside method (Mimms et al., 1981). The tissue factor containing vesicles were sized by gel filtration before use (Reynolds et al., 1983). Greater than 80% of the vesicles were between 100 and 200 nm. Because some tissue factor molecules are trapped inside of vesicles during relipidation (Bach et al., 1986), the effective concentration, that is, the sites available for binding by factor VIIa, is about half the total concentration. The effective concentration was used throughout these studies.

Factor VIIa was derivatized and inactivated by incubation for 5 h with 5 mM DFP obtained from Aldrich Chemicals. The resulting DIP-VIIa had no detectable activity using a conventional coagulation assay (Nemerson & Clyne, 1974) or a radiometric assay (Zur & Nemerson, 1982).

Radiometric assays were employed for all kinetic measurements of the activation of factors IX and X (Zur & Nemerson, 1982). Briefly, the proteins, each of which contains sialic acid, are oxidized with periodate and reduced with tritiated $NaBH_4$ (≈10 Ci/mmol; New England Nuclear, Boston, MA). As the activation of these zymogens is accompanied by the release of a peptide containing about 40–60% of the radioactivity of the zymogen, their activation may be measured by extraction of the peptides into 5% Cl_3CCOH in which neither the zymogens nor the derivative enzymes of the zymogens are appreciably soluble. The radioactivity contained in the Cl_3CCOOH, which is proportional to the extent of zymogen activation, is then estimated by using a Beckman LS7000 spectrometer. Velocities were calculated from a linear least-squares fit using at least seven time points in duplicate. Substrate hydrolysis was less than 10% except when full time courses were evaluated.

Factor Xa causes the release of extraneous counts when factor X is used as the substrate (Silverberg et al., 1977). We previously employed benzamidine to obviate this difficulty. As benzamidine inhibits both factor Xa and factor VIIa, thus complicating the interpretations, we now use isoleucylglutamylglycylarginine chloromethyl ketone (Kettner & Shaw, 1981) to inhibit the spurious reaction. We found that the inclusion of this inhibitor at 1 μM completely blocked the attack of 50 nM factor Xa on 1000 nM factor X (data not shown). When the inhibitor was added to a reaction consisting of tissue factor, factor VIIa, and factor IX, no inhibition was

[1] Abbreviations: DFP, diisopropyl fluorophosphate; DIP, diisopropylphosphoro; Cl_3CCOOH, trichloroacetic acid; enzyme (factor VIIa), activator (tissue factor), and substrate (factor IX or X) are referred to as E, A, or S, respectively, and the total concentrations of these species are subscripted with a "T" whereas the free species are not subscripted.

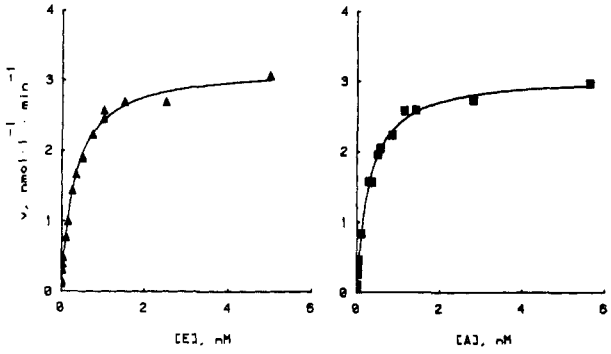

FIGURE 1: Effect of enzyme and activator titrations on the velocity of factor X activation. In the left panel, factor VIIa concentration was raised from zero to 5 nM while tissue factor concentration (phosphatidylcholine) was constant at 0.075 nM. In the right panel, tissue factor concentration was incremented to 6 nM while factor VIIa concentration was 0.075 nM. The substrate concentration was 50 nM.

noted when a similar concentration was employed (data not shown). We interpret this experiment as showing the inhibitor to have no effect on factor VIIa. Accordingly, the chloromethyl ketone was included in all radiometric assays. Porcine intestinal heparin, grade I (176 units/mg), was purchased from Sigma, St. Louis, MO.

Kinetic parameters were calculated by fitting the indicated equations to the data using Marquardt's nonlinear least-squares algorithm (Tektronix, plot 50, vol. 4). No weighting was employed.

RESULTS

A property of an essential activation model is that the total catalytic activity present is limited by the concentration of both enzyme and activator. This phenomenon is demonstrated for a tissue factor dependent reaction in Figure 1 in which enzyme and activator titrations were performed at a constant substrate concentration. In each instance, the fixed ligand concentration, either enzyme or activator, was 0.075 nM. The substrate, factor X, concentration was 50 nM. From these data, it is clear that the velocity in the absence of either E or A is zero and that the velocity achieved as activator or enzyme concentration is raised is limited by the concentration of the reciprocal ligand. This experiment is entirely consistent with a model in which the only catalytic species is the AES complex; i.e., tissue factor is an essential activator.

In order to confirm these impressions, we first derived equations that describe the initial velocity of this system in terms of the total concentrations of enzyme, activator, and substrate (see the Appendix). The derivations describing the initial velocity, v, may be based on either rapid equilibrium or steady-state assumptions.

In model I, the conservation equations for total enzyme and activator, E_T and A_T, are[2]

$$E_T = E + AE + AES \quad (1a)$$

$$A_T = A + AE + AES \quad (2a)$$

We assume that the concentration of free substrate, S, approximates that of the total substrate, S_T:

$$S_T \approx S \quad (3a)$$

In the steady-state analysis of model I, the unidirectional rate constants are explicit. There are, however, two possible

[2] All equations are derived in the Appendix starting from the most general model. The equations are denoted by an Arabic numeral followed by an "a".

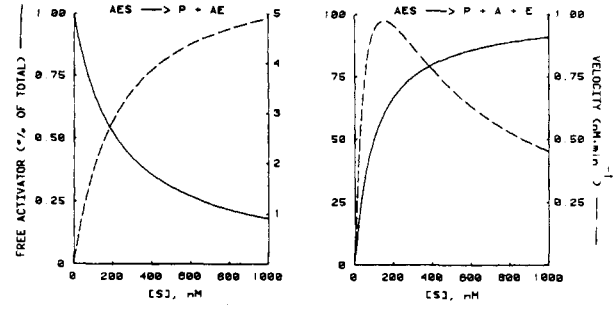

FIGURE 2: Simulation of the two steady-state models II and III. The velocity was calculated from eq 11a by using K_1 and K_{1a} (eq 8a and 15a). Free activator was total activator minus the sum of EA and EAS. The activator concentration was set at 0.025 nM; the enzyme concentration was set at $100K_1$, giving about 1% free activator in the absence of substrate. A value of 220 nM was assumed for K_2; the k_{cat} was 220 min^{-1}, and k_{-1} was 1.1 min^{-1} (see Figure 4).

models corresponding to model I, depending on whether product formation is accompanied by the release of the AE complex or by the release of free E and free A:

$$A + E \underset{k_{+1}}{\overset{k_{-1}}{\leftrightarrow}} AE + S \underset{k_{+2}}{\overset{k_{-2}}{\leftrightarrow}} AES \xrightarrow{k_{cat}} P + AE \quad (II)$$

and

$$A + E \underset{k_{+1}}{\overset{k_{-1}}{\leftrightarrow}} AE + S \underset{k_{+2}}{\overset{k_{-2}}{\leftrightarrow}} AES \xrightarrow{k_{cat}} P + E + A \quad (III)$$

For both model II and model III, the conservation equations are given by eq 1a, 2a, and 3a. The only difference between models II and III lies in the dynamical equations expressing the rate of change of free enzyme and free activator with respect to time. For model II

$$dE/dt = dA/dt = -k_{+1} \cdot E \cdot A + k_{-1}AE \quad (6a)$$

and for model III

$$dE/dt = dA/dt = -k_{+1} \cdot E \cdot A + k_{-1}AE + k_{cat}AES \quad (13a)$$

The steady-state solution for model II is

$$v = 0.5k_{cat}[S/(K_2 + S)][M - SQR(M^2 - 4E_TA_T)] \quad (11a)$$

where $K_1 = k_{-1}/k_{+1}$, $K_2 = (k_{-2} + k_{cat})/k_{+2}$, SQR is the square root function, and $M = A_T + E_T + K_1/(1 + S/K_2)$. Equation 11a is consistent with the data in Figure 1, namely, that in the absence of enzyme or activator, the velocity would be zero. K_2 explicitly contains a kinetic term, k_{cat}, which we later show to be a small contributor to this parameter.

On the other hand, the solution for model III results in eq 11a, but with K_1 in M being replaced by K_{1a}:

$$K_{1a} = K_1[1 + (k_{cat}/k_{-1})(S/K_2)] \quad (15a)$$

The effect of the inclusion of the term $k_{cat}AES$ in eq 13a is obligatory substrate inhibition resulting from the dissolution of the catalytic complex with each product-forming cycle. This is illustrated in Figure 2 in which graphs of the steady-state velocity equations for these models are simulated. As this is contrary to our observations, we can reject model III.

To explore the kinetics of this system, apparent Michaelis–Menten kinetic parameters were estimated from initial velocity data. While the initial velocity equation for model II, eq 11a, cannot be rearranged into the classical Michaelis–Menten form, a fit of this equation to the data is useful for diagnostic purposes. Thus, while the parameters obtained do not have a fundamental significance, we have employed them phenomenologically to indicate the effects of perturbations on the system in "conventional" terms, namely, V_{max} and $K_{m\,app}$. In considering an ordered addition model, it is intuitively

Table I: Kinetic Effects of Monoclonal Anti-Tissue Factor on Factor X Activation[a]

addition	$K_{m\,app}$ (nM)	V_{max} (nM min^{-1})
none	16 ± 3	3.04 ± 0.13
antibody	377 ± 64	3.01 ± 0.18

[a] The reaction mixtures were assembled and allowed to equilibrate at 37 °C for 5 min. The reactions were initiated by the addition of substrate. The conditions used were as follows: tissue factor (10% phosphatidylserine), 0.0125 nM; factor VIIa, 2 nM; monoclonal antibody, 1 μM; $CaCl_2$, 5 mM. Ten substrate concentrations were used for each experiment, the highest being at least 5 times the $K_{m\,app}$. The values are shown ± SE.

obvious that the addition of an antiactivator, a reagent competing for enzyme binding sites on the activator, would raise the $K_{m\,app}$ without affecting the V_{max}. The reason for this is that the addition of substrate would "pull" the equilibria toward the formation of AES complexes at the ultimate expense of the antiactivator–activator complexes.

To demonstrate this phenomenon, we utilized a monoclonal antibody directed against bovine tissue factor. The antibody has been shown to "displace" factors VII and VIIa from the activator and to inhibit the two-stage clotting assay for tissue factor (Carson et al., 1985). The data (Table I) indicate that the antibody (Ab) does, in fact, raise the $K_{m\,app}$ without affecting the V_{max}. Intuitively, this is in accord with the behavior of an ordered addition, essential activation model:

$$\begin{array}{l} A + E \underset{}{\overset{K_1}{\rightleftharpoons}} AE + S \overset{K_2}{\rightleftharpoons} AES \xrightarrow{k_{cat}} P \\ \quad + \\ \quad Ab \\ \quad \alpha K_1 \downarrow \\ \quad AbA \end{array} \qquad \text{(IV)}$$

In model IV, the conservation equations for E_T and S remain the same, i.e., eq 1a and 3a. The conservation equations for Ab_T and A_T are

$$Ab_T = Ab + AbA$$

$$A_T = A + AbA + AE + AES$$

We have derived an algorithm to evaluate the initial velocity for a more complex model which includes model IV as a special case (see Algorithm I in the Appendix). We confirmed the intuitive impression that the $K_{m\,app}$ would rise with increasing Ab concentration by simulating the velocity utilizing algorithm I: the $K_{m\,app}$ rises with Ab concentration with no change being observed in V_{max} (not shown). This is similar to the experimental data shown in Table I, in which the same effects on the parameters are noted.

We previously reported that factors VII and VIIa are inhibited by DFP and that the resultant DIP proteins inhibit the tissue factor pathway (Radcliffe & Nemerson, 1976; Zur et al., 1982). We interpreted the inhibition as arising from the formation of DIP–VIIa–tissue factor complexes; that is, the DIP-VIIa was postulated to function in a manner identical with that of the antibody. A kinetic analysis of the mode of inhibition, however, showed the effect to be due entirely to a decrease in the V_{max} which is, of course, inconsistent with the antibody data presented in Table I. We repeated the previously reported experiment, and the data are unchanged; however, we found that the sequence in which the reactants are added to the reaction has marked effects on the apparent mode of inhibition. The data demonstrating this phenomenon were obtained in two ways. In the first, all the reactants were assembled, and the reaction was initiated with Ca^{2+}. In the second, the reaction was assembled in the absence of the inhibitor and initiated with Ca^{2+}; inhibitor was then added. When the inhibitor is present at zero time, the inhibition is severe and not related to substrate concentration; i.e., the effect is on the V_{max}. Conversely, when the inhibitor is added after the substrate, the inhibition is less severe and does not occur at high substrate concentration; i.e., the effect is limited to the $K_{m\,app}$ (Table II). It is evident that the sequence in which reagents are added to the reaction mixture determines the apparent mode of inhibition.

Table II: Effect of DIP-VIIa on the Kinetic Parameters of Factor X Activation[a]

addition	$K_{m\,app}$ (nM)	V_{max} (nM min^{-1})
none	16 ± 3	3.04 ± 0.13
DIP-VIIa with S	17 ± 2	0.30 ± 0.18
DIP-VIIa after S	180 ± 19	2.98 ± 0.23

[a] The conditions employed were as follows: tissue factor, 0.0125 nM (10% phosphatidylserine); factor VIIa, 2 nM; DIP-VIIa concentration was 20 nM when added after the substrate and 2 nM when added with substrate. Ten substrate concentrations were used with the highest being at least 8 times the $K_{m\,app}$. The control experiment is the same as that shown in Table I.

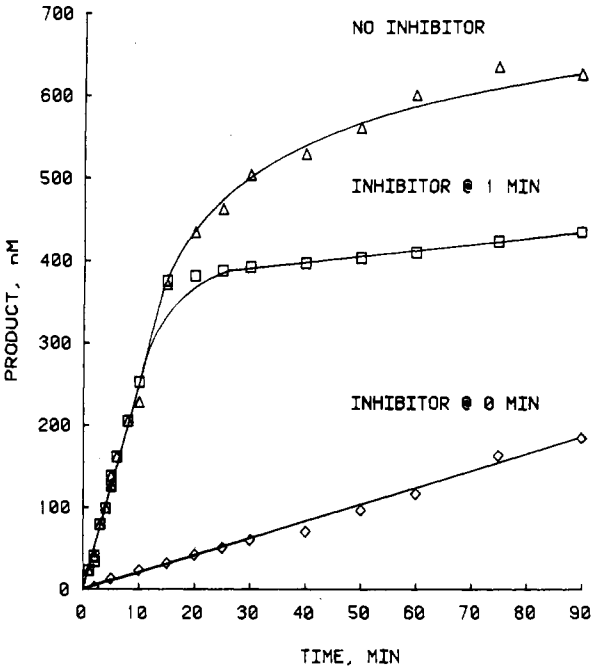

FIGURE 3: Time course of factor IX activation showing the effects of the sequence of addition of reagents on the inhibition induced by DIP-VIIa. The substrate concentration was 1000 nM; tissue factor concentration was 0.1 nM (10% phosphatidylserine), and factor VIIa concentration was 2 nM. DIP-VIIa was used at 20 nM.

In these experiments, the inhibitor was added 1 min after the substrate. Further data, not shown, indicate the velocities to be identical when the inhibitor is added from 10 s to 10 min after the substrate. The duration of these effects is illustrated in Figure 3 in which the reactions are shown over a long time course. It is clear that when the substrate preceded the inhibitor, protection was complete for over 12 min; when the inhibitor was added before the substrate, however, the velocity remained reduced over the course of the experiment.

A hypothesis which could explain this apparent anomaly is that the inhibitor used, DIP-VIIa, has an intact substrate binding site whereas the antibody directed toward tissue factor does not. The essential difference between antibody and DIP-VIIa, then, would be that the latter forms AIS complexes, where I is DIP-VIIa, whereas antibody–activator–substrate

complexes do not form. A model depicting this mechanism for the action of DIP-VIIa is as follows:

$$\begin{array}{ccccccc} A + E & \overset{K_1}{\rightleftharpoons} & AE + S & \overset{K_2}{\rightleftharpoons} & AES & \xrightarrow{k_{cat}} & P \\ + & & & & & & \\ I & & & & & & \\ \alpha K_1 \updownarrow & & & & & & \\ AI + S & & \overset{\beta K_2}{\rightleftharpoons} & & AIS & & \end{array} \qquad (V)$$

where K_1, K_2, and k_{cat} are as described previously and α and β are coefficients relating the constants of the inhibited to the productive pathway in model V. Algorithm I generates the initial velocity for the complete system including the two classes of inhibitors. When the substrate binding site is intact, i.e., when model V pertains, the kinetic consequence of the inhibitor is a decrease in the V_{max}, which is readily demonstrated via simulation of the velocity generated by algorithm I. When the substrate binding site is eliminated (when K4 in algorithm I is set to infinity), the equation describes the inhibition consequent to the antibody which affects the $K_{m\,app}$, a result also confirmed by simulations. When the inhibitor concentration is set to zero, the velocity is described by eq 11a.

On the basis of this model, the results can be explained as follows: when all the reactants are present from time zero, the complexes depicted in model V form as dictated by the appropriate kinetic and equilibrium constants. Alternatively, if the complexes are allowed to form in the absence of inhibitor and the substrate concentration is very high, little free activator would exist, thus precluding significant formation of the inhibitory AI complexes. This means, in effect, that k_{-1} as defined above must be slow relative to the re-formation of AES after product formation; i.e., $k_{+2}S$ must be $>>k_{-1}$. This formulation also predicts that some free A will exist when the substrate concentration is low, thus providing a target for the DIP-VIIa. The data shown in Table II were obtained with limiting concentrations of activator; i.e., the enzyme concentration exceeded that of the activator. Under these conditions, it can be shown that free activator concentration will decline with increasing substrate concentration, the limit being no free activator as substrate concentration approaches infinity. Algebraically, this is demonstrated by taking the limit as S approaches infinity in eq 11a, which then reduces to

$$V_{max} = k_{cat}\min(A_T, E_T) \qquad (54a)$$

This means that at V_{max}, the theoretical maximum velocity, the concentration of AES, the product-forming species, equals, under these experimental conditions, the concentration of A_T, or, in practice, as the velocity approaches V_{max}, the concentration of free A approaches zero. It follows from eq 54a that the reaction velocity would be unaffected by the addition of DIP-VIIa when substrate concentration approached infinity.

At substrate concentrations used experimentally, however, the response of the system to the addition of DIP-VIIa depends on the relative magnitudes of k_{-1} and k_{+2}. We have approached the determination of k_{-1} as follows: tissue factor (0.2 nM) was equilibrated with factor VIIa (10 nM) in the presence of Ca^{2+}. DIP-VIIa (100 nM) was added. Aliquots were withdrawn at the indicated intervals (Figure 4) and assayed following the addition of factor X (1000 nM). As can be seen, the activity decayed over time. The experimental points in Figure 4 were fit to

$$y \approx e^{-kt} + b$$

where y is the activity at time t, k is a first-order rate constant, and b is the value the velocity approaches asymptotically. This equation is only approximate because active enzyme represents

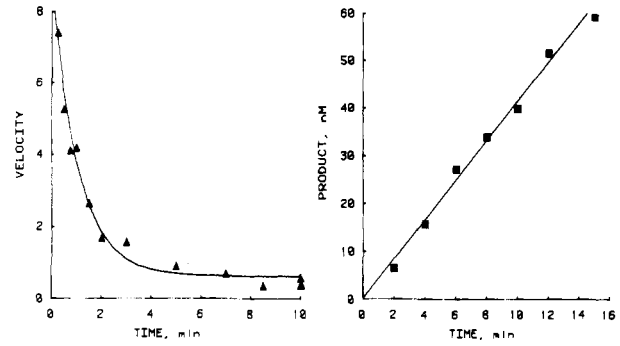

FIGURE 4: Determination of the off rate of factor VIIa from tissue factor (10% phosphatidylserine). Enzyme (10 nM) and activator (0.2 nM) were preincubated in 5 mM $CaCl_2$ for 5 min. DIP-VIIa (100 nM) was added at zero time, and aliquots were removed as indicated and added directly to 1000 nM factor IX for assay. The panel on the left shows the decrease of activity with time. The right panel shows the linear assay obtained when the activity had fallen to about 50% of the starting value.

about 9% of the total ligand which results in some re-formation of AES. The calculated value of b is 0.071 ± 0.016, in good agreement with the fractional concentration of factor VIIa, 0.09. The value of k thus obtained, 1.1 ± 0.16 min^{-1}, approximates k_{-1} but is underestimated by about 9%. Further confirmation of model V, and implicitly model I, is that following the addition of substrate to the reaction the velocities remain linear for about 12 min (Figure 4). That is, substrate blocks the exchange of active enzyme for DIP-VIIa. Expressed differently, on the basis of the values obtained for the off rate, the $t_{1/2}$ for the AE complex is about 38 s, whereas in the presence of substrate full protection is observed for about 12 min, or over 18 half-lives. These observations are in accord with our hypothesis that substrate binding precludes dissociation of free E or free A from AES; i.e., the reaction is ordered. Further, these data support the choice of the corresponding steady-state model (II) which stabilizes the AE complex rather than model III which destabilizes it (see Figure 2).

If, as we suggest, k_{-1} is a slow step, then the velocity obtained by preincubating enzyme and activator at high concentration and then initiating the reaction following a dilution–jump should exceed that obtained in a control reaction. To test this concept, activator and enzyme were incubated in 5 mM Ca^{2+} at 500 times their final concentrations. The mixture was then diluted into 540 nM factor X; at the intervals indicated on Figure 5, aliquots were removed from the assay for estimation of product formation. The results are expressed as the ratio of the product formed in the dilution–jump to that formed in the control experiment. It is evident that the equilibration is fairly slow; the reactions require about 10 min (at which time ~70% of the substrate had been hydrolyzed) to approach similar amounts of product formation.

It now remains to be determined whether in the experimental range of substrate concentrations $k_{+2}S$ is $>>k_{-1}$. We approached this determination by first estimating k_{+2} relative to k_{cat}. To this end, we exploited model V using DIP-VIIa and the property of heparin and some other acidic polysaccharides to stimulate the k_{cat} when factor IX (only) is the substrate (Repke et al., 1981). The general strategy we adopted was to examine changes in the degree of inhibition engendered by DIP-VIIa as large changes in the k_{cat} were introduced. The argument we make is that because K_2 is, in essence, $(k_{-2} + k_{cat})/k_{+2}$, whereas αK_2 is simply an equilibrium term, $\alpha k_{-2}/k_{+2}$ (where α is a pure number), changes in the k_{cat} would unbalance model V, thus changing the degree of

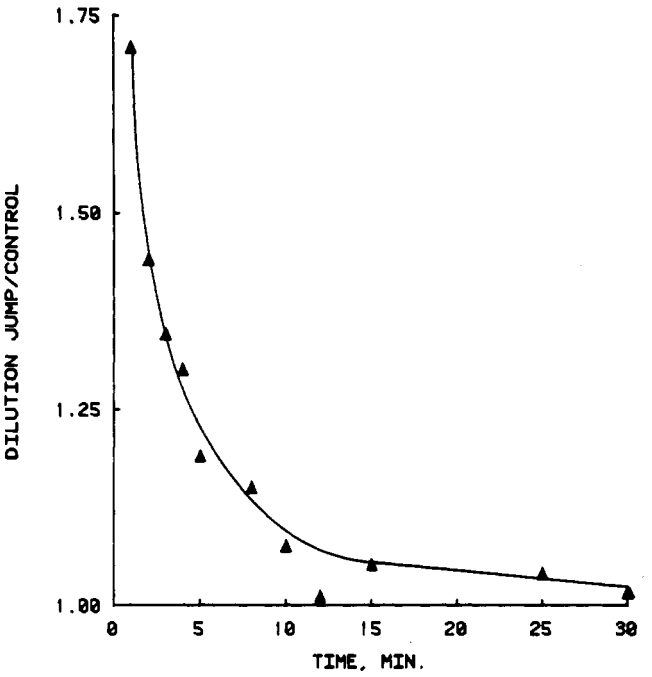

FIGURE 5: Effect of a dilution–jump on product formation. Enzyme and activator (10% phosphatidylserine) were incubated at 500 times their final concentrations in the presence of 5 mM $CaCl_2$. After equilibration for 5 min, the mixture was diluted into 540 nM factor X. The control was treated similarly. The data are expressed as the ratio of the product present at each time in the dilution–jump to that present in the control experiment. At the 30-min point, approximately 70% of the substrate had been hydrolyzed.

Table III: Effect of Heparin on DIP-VIIa-Dependent Inhibition of Factor IX Activation[a]

addition	control	v (nM min^{-1}) +DIP-VIIa, 2.0 nM	% inhibn	v (nM min^{-1}) +DIP-VIIa, 20 nM	% inhibn
none	1.43	0.75	48	0.13	91
heparin	13.90	8.43	40	1.45	90

[a] The conditions used were as follows: tissue factor, 0.2 nM (phosphatidylcholine); factor VIIa, 2.0 nM; factor IX, 1000 nM; DIP-VIIa as shown. Heparin concentration was 2 μM, assuming a molecular weight of 15 000.

inhibition *if* k_{cat} were large with respect to k_{-2}. This would arise because raising the k_{cat} would lead to an effective increase in K_2, thereby favoring the formation of AIS over AES; i.e., the addition of heparin would lead to an increase in the degree of inhibition. In fact, this is contrary to what we observed. In Table III, we show data indicating that increasing the reaction velocity 9.7-fold did not increase the degree of inhibition engendered by DIP-VIIa.

From these data, we conclude that the k_{cat} must be much smaller than k_{-2}. First, if we assume that we could readily detect a 10% change in the degree of inhibition, it follows that the k_{cat} must be no more than 10% as large as k_{-2}. Since the k_{cat} is $\sim$220 min^{-1}, we get a k_{-2} of at least 2200 min^{-1}. Thus, given a K_2 of $\sim$220 nM (see below), this implies a minimum estimate for k_{+2} of about 10 nM^{-1} min^{-1}. As the re-formation of AES is a function of $k_{+2}S$, we conclude that in the experimental range of substrate concentrations, its rate of re-formation after each catalytic cycle is faster than the dissociation of AE into free species.

Quantitative Aspects of the Ordered Addition Model. As shown in the preceding paper (Bach et al., 1986), the binding of enzyme to activator is affected by the composition of the vesicles into which tissue factor is inserted. Because phosphatidylserine induces complex binding isotherms and because the substrates bind to acidic vesicles, thus introducing ambiguities regarding the true substrate concentration, the following experiments were performed utilizing vesicles consisting of phosphatidylcholine. We have generated a set of data consisting of 246 velocity determinations at various enzyme, activator, and substrate concentrations to which we have fit the initial velocity equations of models II and III. The results of a global fit confirm that only model II is consistent with this data set (Table IV). The "goodness of fit" notwithstanding, we emphasize that K_1 was evaluated to be 0.09 nM whereas its value determined from equilibrium measurements is 4.5 nM (Bach et al., 1986). Because of this discrepancy, we have explored further the characteristics of model II. Note that in Table IV, when product formation is accompanied by the regeneration of AE, the equations describing model II return the same values whether derived from steady-state or rapid equilibrium assumptions. Accordingly, we have utilized the algebraically simpler rapid equilibrium derivations in this work. Thus, we will refer only to model I, assuming that each cycle produces AE + P as in model II.

Table IV: Calculated Parameters for Ordered Addition Models II and III[a]

	parameter		
model	K_1 (nM)	K_2 (nM)	k_{cat} (min^{-1})
P + EA (II)	0.09 ± 0.01	283.8 ± 20.1	210.0 ± 4.5
P + E + A (III)	$9 \times 10^{-6} \pm 2 \times 10^{-6}$	478.4 ± 43.5	225.3 ± 8.2

[a] For model III, k_{-1} was set at 1.1 min^{-1}. When k_{-1} was treated as an adjustable parameter, it was evaluated to be $\approx 10^{16}$ min^{-1}, while K_1 was estimated to be 0.031 ± 0.006 nM. Model I yielded the same values when fit to the steady-state velocity equation (eq 11a) or to the rapid equilibrium equation (eq 52a) as derived in the Appendix. One standard error is indicated.

It is intuitively apparent that in model I the concentration of the AE complex is regulated by substrate concentration. This means that the amount of enzyme or activator required to saturate the reciprocal ligand will vary inversely with the substrate concentration. We define V_E and V_A as the maximum velocity achieved at a given substrate concentration as enzyme or activator concentration, respectively, is raised to infinity. The amount of enzyme or activator required to achieve half of the maximum velocity is denoted by $K_{1/2,E}$ or $K_{1/2,A}$, respectively. We derive the expressions for $K_{1/2,E}$; however, as the model is entirely symmetrical with respect to E and A, by substituting A for E, the expression for $K_{1/2,A}$ is readily obtained.

To solve for $K_{1/2,E}$, we first determine the maximum velocity, V_E, obtained when E is raised to infinity in the initial velocity equation (eq 52a), yielding

$$V_E = k_{cat}A_TS/(K_2 + S) \quad (56a)$$

We note parenthetically that as either E or A is raised toward infinity, the resulting equations are similar in form to the Michaelis–Menten equation. Now, to determine $K_{1/2,E}$, we set $v = 0.5V_E$ and solve for E. As shown in the Appendix, this results in the equation:

$$K_{1/2,E} = A_T/2 + K_1K_2/(K_2 + S) \quad (57a)$$

From eq 57a, it is clear that $K_{1/2,E}$ reaches a maximum, $A_T/2 + K_1$, as S approaches zero and that it monotonically declines, reaching the limit of $A_T/2$ as S approaches infinity. Expressions for activator titrations are obtained simply by interchanging E_T and A_T in these equations. The experimental data are portrayed in Figure 6 in which enzyme and activator titrations are shown at two substrate concentrations. To

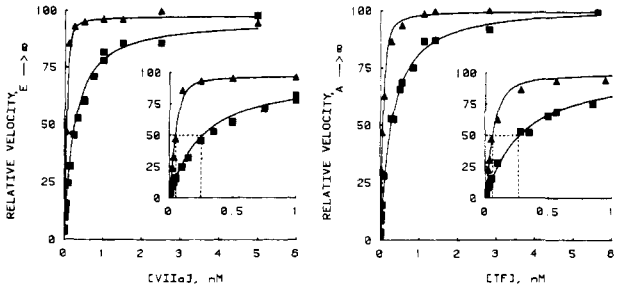

FIGURE 6: Enzyme and activator titrations at equivalent reciprocal ligand concentration. When fixed, the tissue factor (right panel) and factor VIIa (left panel) concentrations were 0.075 nM. The curves are a fit to the initial velocity equation for model 1. The $K_{1/2}$ for each titration was determined by using eq 57a with the values shown for model II (Table IV). For direct comparison, the data were normalized to V_E or V_A. For clarity, the inserts are shown with an expanded scale. The triangles represent data obtained with 2000 nM S and the squares with 50 nM S.

visualize the effects of the substrate on the titrations, all data are normalized to a percent of V_E or V_A. The data shown expanded in the insets clearly demonstrate that increasing the substrate concentration decreases $K_{1/2}$; in this instance, changing the substrate concentration from 50 to 2000 nM decreased the $K_{1/2,E}$ from 0.296 to 0.046 nM and the $K_{1/2,A}$ from 0.316 to 0.060 nM, a decrease of 84% and 88%, respectively.

To derive an expression for the $K_{m\,app}$, we first solve for the substrate concentration resulting in $v = 0.5V_{max}$. This yields

$$K_{m\,app} = K_2[B_1 - \mathrm{SQR}(B_1^2 - L_1B_2)]/B_2 \qquad (55a)$$

where

$$L_1 = \min(E_T, A_T)$$

$$L_2 = \max(E_T, A_T)$$

and

$$B_1 = K_1 + L_2 \quad \text{and} \quad B_2 = 2L_2 - L_1$$

From eq 55a, it is obvious that the $K_{m\,app}$ is not a single constant but rather a function of E_T and A_T. Simulation of the function (Figure 7) shows that the $K_{m\,app}$ reaches a maximum when $A_T = E_T$ and asymptotically approaches a minimum, K_2, when either E_T or A_T gets very large with respect to its reciprocal ligand. We have determined the $K_{m\,app}$ at a constant activator concentration, 0.025 nM, while varying the enzyme concentration from 0.0125 to 20 nM. The data (Figure 8) show that in a qualitative sense, the observed values agree with the simulations; i.e., the expected cuspid behavior is observed. However, when eq 55a was fit to the data shown in Figure 8, K_2 was estimated to be 401 ± 106 nM while we have observed several values well below this; further, K_1 evaluates to 0.04 ± 0.02 nM, again very different from the 4.5 nM determined directly.

The V_{max}, extracted from the same data, reaches a level after which it does not substantially change even though the enzyme concentrations increase another 160-fold (Figure 9). We recognize that there is a small positive slope to the data as E_T increases, although the change is less than 10%. While it is possible that this might reflect a fundamental phenomenon, we consider it more likely that it results from the difficulty in achieving substrate concentrations high enough to accurately calculate V_{max}.

Because of the discrepancies regarding K_1, we have explored the other possible essential activation models involving a ternary complex of E, A, and S to determine if the apparent tight binding of enzyme could be explained by a different

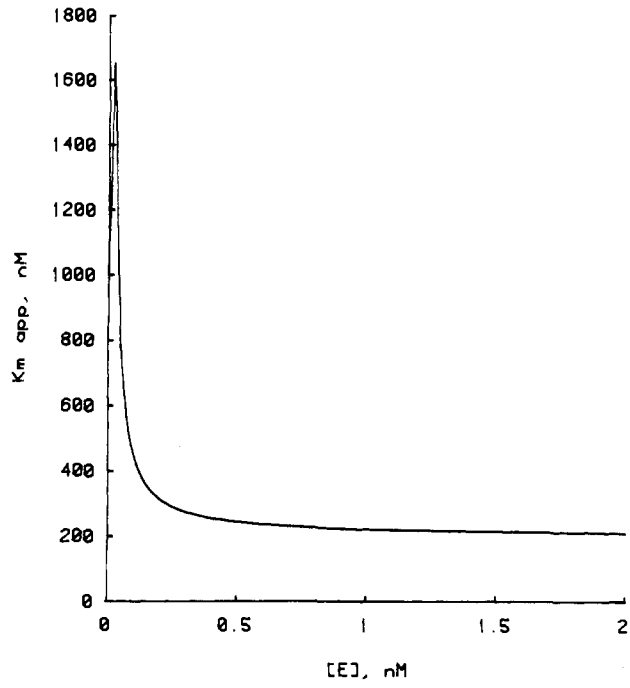

FIGURE 7: Simulation of the $K_{m\,app}$ function for model II. The parameters used were from Table IV, model II.

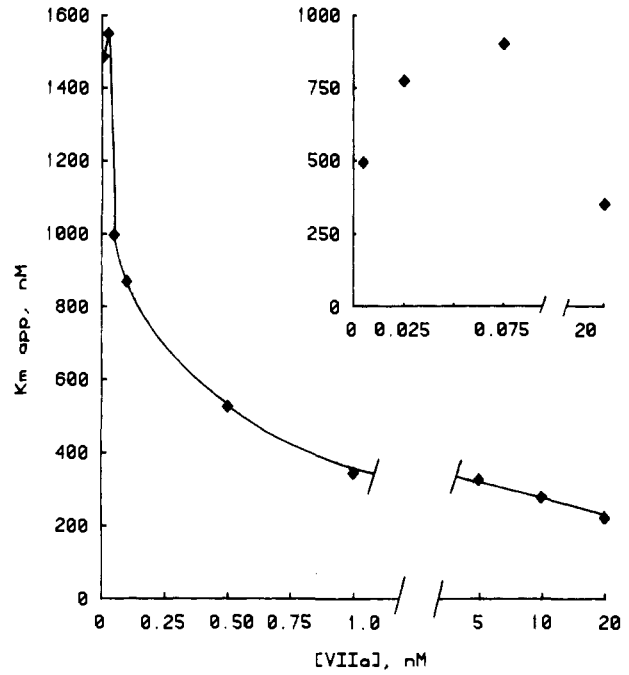

FIGURE 8: Experimentally determined $K_{m\,app}$ as a function of enzyme concentration. The larger data set was obtained by using 0.025 nM tissue factor. To visualize the ascending limb, several points obtained with 0.075 nM tissue factor (inset) are shown. The standard errors of these determinations averaged approximately 10%.

kinetic mechanism.

The full random model with one catalytic species, AES, is

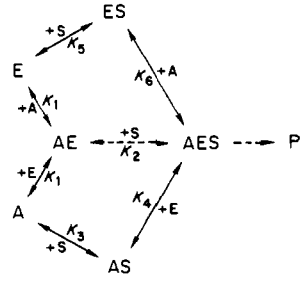

(VI)

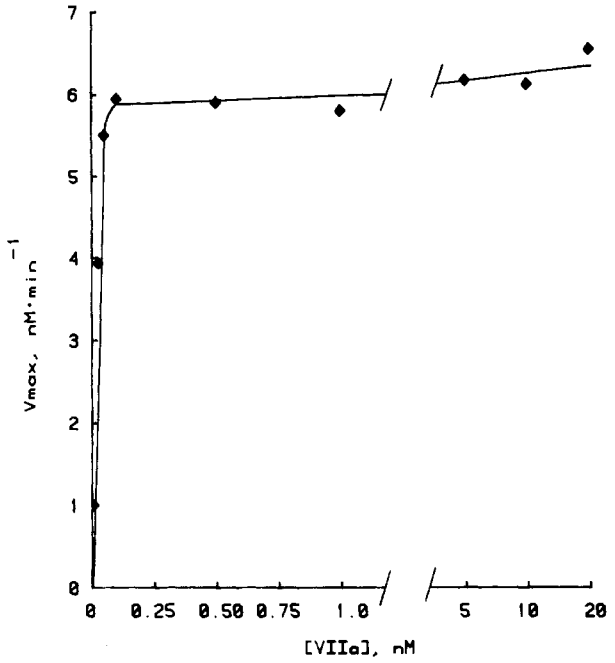

FIGURE 9: Experimentally determined V_{max} shown as a function of enzyme concentration. The same experimental data as shown for Figure 8 were utilized (0.025 nM tissue factor only). The nominal equivalence point would lie just below the third data point.

In this model, ES and AS species exist in addition to the species shown in model I. A numerical solution of the velocity equation (eq 50a) as a function of substrate concentration indicates severe substrate inhibition resulting from the formation of binary ES and AS complexes at the ultimate expense of the product-forming AES. Further simulations show that as substrate concentration rises, the $K_{1/2,E}$ and $K_{1/2,A}$ *also rise.* As both the substrate inhibition and the effects of substrate on enzyme and activator titrations are not in accord with our data, we can reject the full random model.

In a partial random model, in which AS but not ES complexes form, the addition of the new binding site can either increase or decrease the $K_{1/2,E}$ depending on the magnitude of the equilibrium constants. The expression for $K_{1/2,E}$ is

$$K_{1/2,E} = A_T/2 + K_1(1 + S/K_3)/(1 + S/K_2) \quad (64a)$$

The limit of eq 64a as S approaches infinity is

$$\lim_{S\to\infty} K_{1/2,E} = A_T/2 + K_4 \quad (65a)$$

The enzyme titration data shown in Figure 6 yield a $K_{1/2,E}$ of 0.046 nM at a substrate concentration of 2000 nM and a tissue factor concentration of 0.075 nM. As $A_T/2$ equaled 0.038 nM, this gives an upper bound for K_4, describing the dissociation of AES to E + AS, of 0.01 nM. From eq 62a, it follows that the $K_{m\,app}$, when $E >> K_1$, is equal to K_2. Since we have measured a $K_{m\,app}$ of about 200 nM at high enzyme concentration, we use this value as a reasonable estimate of this parameter. Taking K_1 to be 4.5 nM and using the equilibrium relationships, we calculate that K_3, describing the dissociation of AS, has a value of at least 100 000 nM. Therefore, at a substrate concentration of 1000 nM, substrate will occupy only 1% of the total activator. Thus, it is clear that even at relatively high substrate concentrations the AS complex would be insignificant. This phenomenon is reflected in the poor fit obtained when utilizing the velocity equation (eq 59a) for this model: e.g., K_2 evaluates to 6225 ± 14 247 nM and k_{cat} to 223 ± 4691 min^{-1}. From these considerations, we conclude that the fundamental reaction mechanism is fully ordered, the discrepancy in K_1 notwithstanding. Because of symmetry, the alternate partial random model in which ES (but not AS) complexes form behaves identically (when E and A are interchanged in the appropriate equations).

An Alternative, Ordered Addition, Essential Activation Model. We have shown previously that each catalytic cycle results in the formation of product and the AE complex. We suggest that the reason that AE does not dissociate while resident in the AES complex is that substrate induces a change in the binding sites or binding parameters between the two ligands. We designate the altered species as AE*. The complete model illustrating the relations between the species is as follows:

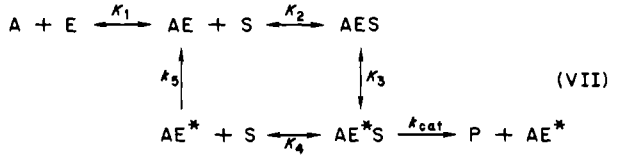

(VII)

In this model, K_1, K_2, and K_4 are equilibrium dissociation constants, and K_3 is an equilibrium conformational constant. We show a unidirectional rate constant, k_5, describing the relaxation of AE* to AE. The essence of model VII which explicitly includes a substrate-induced conformationally transformed species, AE*, is that this species persists for a finite time after product formation, thus allowing the direct re-formation of AE*S. The persistence of this additional species would result in an apparent binding of enzyme to activator which is tighter than that observed in the absence of substrate, i.e., the equilibrium value of K_1 determined directly.

If we had not explicitly included the unidirectional rate constant, k_5, the relationships in model VII would result in an equilibrium between AE and AE*, thus implying the formation of some AE* in the absence of substrate. In this event, we would replace the rate constant k_5 with the dissociation constant K_5. If the transition of AE to AE* is truly reversible, then the estimate, K_1*, of K_1 measured in the absence of substrate is related to the true constant K_1 by

$$K_1 = K_1^*(1 + 1/K_5)$$

Because we have no independent estimate of K_1* and therefore do know how much AE* is formed in the absence of substrate, we cannot fit the velocity equation for model VII (eq 71a) to the data because due to the nonuniqueness of the parameter identification the fit has an infinite number of solutions. The equilibrium model, however, can be tested as follows: using the equilibrium relations, we have derived expressions which relate the $K_{m\,app}$ obtained when E and A are equimolar to that obtained when the enzyme is in large excess. We denote these terms as $K_{m\,app,L}$ and $K_{m\,app,\infty}$, respectively. Consider the ratio, R_{K_m}, of the $K_{m\,app}$ when E_T and A_T are equimolar with the concentration L, $K_{m\,app,L}$, to the limit of the $K_{m\,app}$ as $E \to \infty$, that is, when $E_T >> A_T$, $K_{m\,app,\infty}$:

$$R_{K_m} = K_{m\,app,L}/K_{m\,app,\infty}$$

As shown in the Appendix, assuming that AE and AE* are in equilibrium, it follows that

$$R_{K_m} = (1 + K_1^*/L) + \mathrm{SQR}[(1 + K_1^*/L)^2 - 1] \quad (76a)$$

where L is the concentration of the equimolar E and A.

Our observed value for R_{K_m} is approximately 10 when L = 0.025 nM (see Figure 8). Using these values and solving the above equation for K_1* yield the estimate of ~0.1. As K_1* is greater than K_1, this is inconsistent with the measured value of K_1, 4.5 nM. Similarly, using the measured value of 4.5 nM

as a lower bound for K_1^* generates an estimate of R_{K_m} of >360 which is much larger than the observed ratios. On these grounds, we can reject the full equilibrium version of this model. Put differently, in model VII k_5 can only be a unidirectional rate constant.

Discussion

In this paper, we propose that the fundamental kinetic mechanism regulating the tissue factor dependent coagulation reactions is the ordered addition of reactants. By this, we mean that the enzyme, factor VIIa, binds to tissue factor, an essential activator. This complex then combines with substrate, forming the central, product-forming species. An equivalent statement is that the only physical species present to a significant extent are the free forms of enzyme, activator, and substrate as well as enzyme–activator and enzyme–activator–substrate complexes.

Our model contains, in essence, a series of linked pseudo-equilibria in which the concentration of any species *perforce* regulates the concentration of all other species. To explore this reaction, we used a monoclonal antibody directed toward the enzyme binding site on tissue factor as a mechanistic probe. This antibody, which has been shown to "displace" the enzyme from tissue factor, would, in the absence of substrate, reduce the AE concentration. In an ordered addition model, however, substrate would "pull" the equilibria in the direction of substrate complexes, thus mitigating the effect of the antibody. Indeed, we show (Table I) that the antibody raises the $K_{m\,app}$ of the reaction without affecting the V_{max}, a result predicted by the ordered addition model.

In the ordered addition model, the dissociation AES → A + ES is explicitly forbidden. While this must be so to preserve microscopic reversibility, the inclusion of a substrate-induced conformational change in the AE complex provides a structural explanation for the ordered association and dissociation of this model. In a truly ordered mechanism such as we propose, that is, one in which there are no physical interactions between substrate and activator, a change in the enzyme is a way to explain the forbidden dissociations. We therefore extend the ordered addition model to explicitly include a substrate-induced transient in the AE complex to account for the lack of dissociation of AE while it is resident in the AES species. We refer to the altered, transiently nondissociable species as AE*. In addition, we postulate that following either catalysis or dissociation of substrate from AE*S the same AE* species is generated. AE* does not dissociate directly into free enzyme and activator but rather first "relaxes" into the dissociable AE form. It is the persistence of the AE* species that accounts for the binding of A and E appearing tighter than predicted from a simple ordered addition model. If AE* per se exists and is not included in the conservation equations for model I, then the kinetic equations will evaluate K_1 to be lower than, in fact, it is. Put differently, if AE* relaxed to AE instantaneously upon release of product or substrate, the dissociation constant obtained kinetically and under equilibrium conditions would agree—models I and VII would be indistinguishable. The proposed model, which explicitly indicates AE* → AE to be unidirectional, requires a full set of differential equations for its solution. Using this approach, we find the model does behave appropriately. Because 10 independent rate constants must be evaluated, the actual fit to data is a nontrivial problem which we are currently studying in our laboratories. We do note, however, that while we have no direct evidence that substrate binding increases the affinity of E for A, DIP-VII and DIP-VIIa bind more tightly to tissue factor than do their unconjugated counterparts (Bach et al., 1986).

We have considered the other possible ordered addition models. The only substantially different alternative is when substrate combines with activator, forming the true substrate which is then attacked by free enzyme. In this model, the dynamical equation describing the steady-state concentration of free enzyme contains three terms: $-k_{+1}\cdot E\cdot AS$, $+k_{-1}AES$, and $+k_{cat}AES$, where k_{+1} and k_{-1} are unidirectional on and off rate constants, respectively. Accordingly, each catalytic cycle would produce product, and free enzyme and activator and the model would demonstrate severe substrate inhibition for the same reasons as model III. Another type of ordered addition model would involve the formation of ES complexes as the substrate for the activator. Due to the symmetry of the models, this would behave the same as when AS is the substrate. Further, for both situations, because free activator would be formed with each catalytic cycle, the reaction would be liable to inhibition by DIP-VIIa even when the substrate preceded the inhibitor.

The substrate-induced protection against inhibition by DIP-VIIa, while dramatic, is also transient. As shown in Figure 3, in the presence of 1000 nM factor X, no inhibition is detectable for about 12 min after which the reaction abruptly slows. While the kinetic constants regulating this phenomenon have not yet been determined, this type of transient sequence of addition anomaly is demonstrative of a hysteretic reaction, further evidence for which is presented in Figure 5 where it is shown that the velocity of the reaction is greater when enzyme, activator, and calcium ions are incubated at a high concentration and then added with a dilution–jump to substrate, the initial product formation being some 70% greater compared with a reaction assembled without the dilution–jump. Over time, however, the products formed in the two reactions slowly coverge. This behavior is consistent with the relatively slow k_{-1}; i.e., the hysteresis is due to a slow release of a ligand, in this instance enzyme from activator.

These considerations notwithstanding, equations describing the initial velocity can be applied as long as no perturbations are introduced to the reaction in progress. Because the initial velocity is assumed to be an instantaneous event, hysteresis per se does not compromise the initial velocity equations. Integration of these equations over time, however, would be invalid.

Our proposed model, taken in its entirety, involves two related ligand-enhanced conformational activations. While we have no structural studies to delineate the precise effect of the interaction of tissue factor and factor VIIa, it is clear that in the absence of tissue factor little or no catalysis takes place. We assume, therefore, that upon binding of enzyme to tissue factor, binding sites are created on the enzyme allowing catalytically productive interaction with the substrate, factor X. An alternative and kinetically indistinguishable formulation would involve the enzyme and activator forming a binding pocket for the substrate. As this would require that the enzyme and activator each have *no* affinity for the substrate, we consider this a less likely, although plausible, mechanism. Previous data from this laboratory showed that a general activation is not induced by tissue factor because little or no effect is seen with ester substrates or pseudosubstrates (Jesty & Nemerson, 1974; Zur & Nemerson, 1978). Thus, it appears reasonable to invoke an activator-induced change in the enzyme resulting in sites specific for the protein substrates, factors IX and X. We also postulate that in a reciprocal manner substrate induces a change in the enzyme resulting in much tighter binding to the activator, thereby accounting for both the ordered addition model and discrepant

binding constants. Thus, we envision the ternary AE*S complex as consisting of a "conformational cage" from which enzyme cannot escape until substrate is depleted. In a physiological sense, this appears to be an efficient mechanism as factor VIIa would remain associated with tissue factor until the local concentration of substrate was reduced. Then, and only then, factor VIIa would diffuse away from its membrane-bound activator. Catalysis would then cease because free enzyme does not possess significant coagulant activity.

We wish to emphasize that the effects we have observed such as the $K_{m\,app}$ being a function of enzyme and activator concentrations can only be seen when the lesser ligand is not saturated with its reciprocal speices. We note that in other papers dealing with the kinetics of the tissue factor pathway both from this laboratory (Silverberg et al., 1977) and from others (Morrison-Silverberg & Jesty, 1981) the enzyme was saturated with activator. Under these conditions, the resulting velocity equation (eq 56a) is similar in form to the Michaelis–Menten equation, thereby accounting for the "straightforward" published data.

By virtue of utilizing uncharged phospholipids in the present experiments, we have been able to address the fundamental enzymology of the tissue factor system without regard to the effect of substrate binding to the vesicles. In addition, as tissue factor is at least partly a cell-surface molecule, it seems reasonable to investigate the behavior of the system in which the phospholipids more closely approximate those present on plasma membranes. We have also found the presence of charged lipids markedly complicates the interaction of enzyme and activator. Indeed, the inclusion of phosphatidylserine in the vesicles alters the binding parameters of these constituents, induces cooperativity (Bach et al., 1986), and imparts condition-specific effects on the catalytic rate constant (unpublished data). To distinguish the fundamental enzymology from these secondary effects and the postulated "concentrating" ability of acidic lipids on the substrates, the quantitative aspects of these reactions were explored with uncharged vesicles.

It is generally thought that in addition to the tissue factor pathway, two other coagulation reactions exhibit a lipid dependency: the activation of factor X by factors IXa and VIIIa and the conversion of prothrombin to thrombin catalyzed by a complex of factors Xa and Va ("prothrombinase"). With respect to the activation of factor X, little data exist, but the mechanism does involve an activator, factor VIIIa, which vastly enhances catalysis (Hultin & Nemerson, 1978). With regard to prothrombin activation, the proposed models include factor Va as an enzyme activator although some activity is observed in its absence (Milstone et al., 1971). The recently reported kinetic experiments, however, have generally utilized constant concentrations of enzyme and activator and hence do not address the mechanisms we propose. Indeed, these experiments have focused almost entirely on the role of charged phospholipids in delivering substrate to the membrane-bound enzyme–activator complex (Nesheim et al., 1984; Pusey & Nelsestuen, 1983; van Rijn et al., 1984).

It is clear, however, that all the ways in which enzyme, activator, and substrate can assemble in any essential activation model are included in the equations describing the full random model which encompasses all possibilities involving stoichiometries of 1:1:1 in the catalytic complex. We cannot, however, relate our models to prothrombin activation because the latter reaction is more complicated because the activator, factor Va, dissociates from the surface of the vesicles (van de Waart et al., 1983) and thus an additional species and its dissociation constant must be included in the models. Further, the published data appear to be in conflict: e.g., prothrombin has been shown to enhance factor Xa binding to platelets where the binding site is thought to be factor Va (Millitich et al., 1978). On the other hand, prothrombin implicitly has been held to have no effect on enzyme–activator interactions as the equations describing enzyme and activator titrations contain no substrate term (Nesheim et al., 1979). Until extensive experiments relating velocity to enzyme, activator, and substrate concentrations are reported, the relevance of our models to other coagulation reactions will be unclear.

Acknowledgments

We are grateful to Drs. Eliot Shaw and Charles Kettner for their gift of chloromethyl ketones and to Douglas MacLean for his excellent technical assistance.

Appendix

The appendix presents the derivation of the basic kinetic equations describing the various models discussed in the text. Four separate derivations are presented: the steady-state equations for the ordered addition models; the equations for a simple ordered model with an activator inhibitor; the kinetic equations for a full random enzyme–activator–substrate model (from which the ordered addition and partially ordered addition models are obtained as special cases); and a conformational transition model.

Steady-State Derivation

Derivation of the Velocity Equations for Models II and III. The conservation equations are

$$E_T = E + AE + AES \tag{1a}$$

$$A_T = A + AE + AES \tag{2a}$$

and we assume

$$S_T \approx S \tag{3a}$$

For model II, the dynamical equations that express the rate of change of the constituents with respect to time are

$$dAES/dt = k_{+2}\cdot AE\cdot S - (k_{cat} + k_{-2})AES \tag{4a}$$

$$dAE/dt = k_{+1}\cdot E\cdot A - (k_{-1} + k_{+2}S)AE + (k_{-2} + k_{cat})AES \tag{5a}$$

$$dE/dt = dA/dt = -k_{+1}\cdot EA + k_{-1}AE \tag{6a}$$

The steady-state assumption is that each of these derivatives equals zero. Equating eq 4a to zero gives

$$AE\cdot S/AES = (k_{cat} + k_{-2})/k_{+2} \tag{7a}$$

which we define as K_2. Equating eq 6a to zero yields

$$E\cdot A/AE = k_{-1}/k_{+1} \tag{8a}$$

which we define as K_1. Replacing the right side of eq 7a with K_2 and the right side of eq 8a with K_1 yields equations identical with those used to describe the dissociation constants of model I.

To derive the velocity equation, we replace AES by $AE\cdot S/K_2$ in the conservation equations for E_T and A_T. Then we solve simultaneously these two equations with eq 7a to determine the concentration of AE:

$$AE = 0.5[M - \mathrm{SQR}(M^2 - 4E_TA_T)]/(1 + S/K_2) \tag{9a}$$

where

$$M = E_T + A_T + K_1/(1 + S/K_2)$$

Substituting this into the fundamental velocity equation

$$v = k_{cat}AES = k_{cat}\cdot AE\cdot S/K_2 = k_{cat}\cdot A\cdot E\cdot S/K_1K_2 \tag{10a}$$

results in the velocity equation in terms of total enzyme, activator, and substrate:

$$v = 0.5k_{cat}[S/(K_2 + S)][M - \mathrm{SQR}(M^2 - 4E_TA_T)] \quad (11a)$$

where M is as described above.

The other possible steady-state formulation for the fully ordered model assumes that each catalytic cycle produces product plus free enzyme and free activator. For model III, the velocity equation is derived by using eq 4a along with the dynamical equations

$$dAE/dt = k_{+1}\cdot E\cdot A - (k_{-1} + k_{+2}S)AE + k_{-2}AES \quad (12a)$$

$$dE/dt = dA/dt = -k_{+1}\cdot E\cdot A + k_{-1}AE + k_{cat}AES \quad (13a)$$

The steady-state assumption applied to eq 4a results again in eq 7a which, combined with eq 8a set equal to zero, yields

$$E\cdot A/AE = (k_{-1}/k_{+1}) + k_{cat}S/K_2k_{+1} \quad (14a)$$

The right side of eq 14a may be denoted by

$$K_{1a} = K_1[1 + (k_{cat}/k_{-1})(S/K_2)] \quad (15a)$$

Therefore, the steady-state initial velocity for this model is given by eq 11a with K_1 being replaced by K_{1a}, that is, with

$$M = E_T + A_T + K_1[1 + (k_{cat}/k_{-1})(S/K_2)]/(1 + S/K_2) \quad (16a)$$

Kinetic Equations for Ordered Model with Activator Inhibitors

Derivation of the Velocity Equation for Model V. Model V is an ordered addition, essential activation model containing an inhibitor that binds to both substrate and activator. The conservation equations for this model are eq 1a and

$$A_T = A + AI + AIS + AES \quad (17a)$$

$$I_T = I + AI + AIS \quad (18a)$$

Using the equilibrium relations $K_1 = E\cdot A/AE$, $\alpha K_1 = A\cdot I/AI$, $K_2 = AE\cdot S/AES$, and $\beta K_2 = AI\cdot S/AIS$, eq 1a, 17a, and 18a are solved simultaneously for free E, A, and I in terms of their respective total species. To simplify the notation, we introduce two variables:

$$S_1 = (1 + S/\beta K_2)/\alpha K_1 \quad (19a)$$

$$S_2 = (1 + S/K_2)/K_1 \quad (20a)$$

Free I and E are given in terms of free A by

$$I = I_T/(1 + A\cdot S_1) \quad (21a)$$

$$E = E_T/(1 + A\cdot S_2) \quad (22a)$$

Free A is determined as a root of the cubic equation

$$(S_1S_2)A^3 + [S_1 + S_2 + S_1S_2(E_T + I_T - A_T)]A^2 + [1 + S_1(I_T - A_T) + S_2(E_T - A_T)]A - A = 0 \quad (23a)$$

Equation 23a is not factorable; thus, no explicit closed-form solution is possible; but using Newton's method, it can be numerically solved. The numerically determined value of A may be substituted into eq 22a to obtain E. These values for E and A may then be substituted in eq 10a, yielding a value for the initial velocity.

The algorithm used for either curve fitting or simulation of the velocity function follows. It is written in Basic and may be incorporated either into an X–Y plotting routine or into a nonlinear least-squares program. For simulation studies, numerical values are assigned to the parameters.

ALGORITHM I

```
100  REM This algorithm returns the initial velocity as Y1.
       The basic parameters (all as in model V are equi-
       librium parameters K1 and K2, inhibition pathway
       factors α and β, denoted by K3 and K4, respectively,
       and the catalytic parameter k_cat denoted by K. The
       algorithm assumes that the experimental input data
       consist of a matrix X(I,J) where I refers to the ex-
       periment number and the columns contain the sub-
       strate, enzyme, and activator concentrations. The
       inhibitor data are supplied via the code. The al-
       gorithm uses Newton's method to solve a cubic for
       free A (A2) and free E (E1). The tolerance is set
       in line 370 to 0.00001.
110  REM If no AIS is formed, i.e., model IV pertains, K4
       would approach infinity. In this case, set J1 =
       1/(K1·K3) in line 260.
120  REM      ***Parameter Input***
130  K1 = abs(C(1))
140  K2 = abs(C(2))
150  K3 = abs(C(3))
160  K4 = abs(C(4))
170  K = C(5)
180  REM      **A9 = activator concentration**
190  A9 = X(I,3)
200  REM      **E9 = enzyme concentration**
210  E9 = X(I,2)
220  REM      **S9 = substrate concentration**
230  S9 = X(I,3)
240  REM      **I8 = inhibitor concentration**
250  I8 = 0.1
260  J1 = (1+S9/(K2·K4))/(K1·K3)
270  J2 = (1+S9/K2)/K1
275  REM      **Newton's Method To Solve Cubic**
280  A2 = A9
290  A1 = A2
300  D0 = -A9
310  D1 = 1+J1·(I8-A9)+J2·(E9-A9)
320  D2 = J1+J2+J1·J2·(E9-A9+I8)
330  D3 = J1·J2
340  D4 = ((D3·A1+D2)·A1+D1)·A1+D0
350  D5 = (3·D3·A1+2·D2)·A1+D1
360  A2 = A1-D4/D5
370  If ABS(A2-A1)>10^-5 THEN 290
375  REM      **A2 = free activator; E1 = free enzyme**
380  E1 = E9/(1+A2·J2)
390  Y1 = K·E1·A2·S9/(K1·K2)
400  Return
```

Full Random Model

Initial Velocity Equation. The equilibrium dissociation constants for model VI are

$$K_1 = E\cdot A/AE \quad (24a)$$

$$K_2 = AE\cdot S/AES \quad (25a)$$

$$K_3 = A\cdot S/ES \quad (26a)$$

$$K_4 = AS\cdot E/AES \quad (27a)$$

$$K_5 = E\cdot S/ES \quad (28a)$$

$$K_6 = ES\cdot A/AES \quad (29a)$$

The conservation equations are

$$E_T = E + AE + ES + AES \quad (30a)$$

$$A_T = A + AE + AS + AES \quad (31a)$$

As in the models above, we assume that $S_T \approx S$. As this is an essential activation model, we assume only one catalytic species, the AES complex. The fundamental velocity equation

is simply the same as that for the ordered addition, essential activation model, $v = k_{cat}AES$ as given in eq 10a. From the equilibrium relations, the free concentrations of the species are related to AES by

$$E = AE \cdot K_1/A = AES \cdot K_1 \cdot K_2/A \cdot S \quad (32a)$$

$$AE = AES \cdot K_2/S \quad (33a)$$

$$ES = AES \cdot K_6/A \quad (34a)$$

$$AS = AES \cdot K_4/E \quad (35a)$$

$$A = AE \cdot K_1/E = AES \cdot K_1 \cdot K_2/E \cdot S \quad (36a)$$

Substituting these into the conservation equations yields, after factoring:

$$E_T = AES[(1 + K_6/A) + (1 + K_1/A)(K_2/S)] \quad (37a)$$

$$A_T = AES[(1 + K_4/E) + (1 + K_1/E)(K_2/S)] \quad (38a)$$

Equations 37a and 38a are solved simultaneously with

$$AES = E \cdot A \cdot S/K_1K_2 \quad (39a)$$

The algebra and resulting equations are simplified by introducing new variables:

$$S_2 = 1 + K_2/S \quad (40a)$$

$$S_4 = K_4 + K_1K_2/S \quad (41a)$$

$$S_6 = K_6 + K_1K_2/S \quad (42a)$$

$$W = AES \quad (43a)$$

With this notation, the equations to be solved are of the form

$$E_T = W(S_2 + S_6/A) \quad (44a)$$

$$A_T = W(S_2 + S_4/E) \quad (45a)$$

$$W = E \cdot A \cdot S/K_1K_2 \quad (46a)$$

Solving eq 44a and 45a for A and E, respectively, and substituting in eq 46a result, after some algebraic simplification, in an equation quadratic in W:

$$W^2 - (A_T + E_T + S_6S_4S/K_1K_2S_2)W/S_2 + E_TA_T/S_2^2 = 0 \quad (47a)$$

The root of this equation consistent with W being 0 when E_T or A_T is 0 is

$$W = 0.5[R - \mathrm{SQR}(R^2 - 4E_TA_T)]S_2 \quad (48a)$$

with

$$R = A_T + E_T + (S_6S_4S/K_1K_2S_2) \quad (49a)$$

A further algebraic simplification results by denoting the bracketed term in eq 49a by S_9. With this substitution, the velocity equation for the full random model has the form

$$v = 0.5k_{cat}[S/(K_2 + S)] \times \{E_T + A_T + S_9 - \mathrm{SQR}[(E_T + A_T + S_9)^2 - 4E_TA_T]\} \quad (50a)$$

where

$$S_9 = (SK_6 + K_1K_2)(SK_4 + K_1K_2)/[(SK_1 + K_1K_2)K_2] \quad (51a)$$

(*A*) *Ordered Addition Model I.* (*1*) *Initial Velocity.* The conservation equations are the same as for the steady-state model considered above, eq 1a, 2a, and 3a. The derivation of the initial velocity equations for model I is accomplished by making an appropriate choice for specific constants in the equations derived above for the fully random model. The initial velocity equation is given by eq 50a with K_6 and K_4 set to zero in eq 51a. The resulting equation is

$$v = 0.5k_{cat}[S/(K_2 + S)][M - \mathrm{SQR}(M^2 - 4E_TA_T)] \quad (52a)$$

where

$$M = E_T + A_T + K_1K_2/(K_2 + S) \quad (53a)$$

which is identical with the equation derived from the steady-state assumptions in eq 11a.

(*2*) *Maximum Velocity.* Similarly, the V_{max} for the ordered model is obtained from eq 52a and 53a by letting S approach infinity. The ordered addition model is completely symmetric in E_T and A_T, resulting in

$$V_{max} = k_{cat}\min(E_T,A_T) \quad (54a)$$

(*3*) $K_{m\,app}$. The $K_{m\,app}$ equation is obtained by solving $v = 0.5V_{max}$ for S; the symmetry of this model again leads to an expression symmetric in E and A, as follows. First set

$$L_1 = \min(E_T,A_T)$$

$$L_2 = \max(E_T,A_T)$$

and

$$B_1 = K_1 + L_2 \quad \text{and} \quad B_2 = 2L_2 - L_1$$

Then the equation for $K_{m\,app}$ is given by

$$K_{m\,app} = K_2[B_1 - \mathrm{SQR}(B_1^2 - L_1B_2)]/B_2 \quad (55a)$$

While the expression for $K_{m\,app}$ is not as simple as one might desire, its graph as a function of E_T exhibits the observed cuspid property: when initially $E_T < A_T$, the graph is concave upward, increasing until $E_T = A_T$ and then decreasing when $E_T > A_T$. Again, due to the symmetry of this model, A_T and E_T may be interchanged.

(*4*) *Enzyme Titration.* The maximum velocity as enzyme approaches infinity as a function of A_T and S is given by taking the limit as E_T approaches infinity in eq 52a:

$$V_E = k_{cat}A_TS/(K_2 + S) \quad (56a)$$

Solving $v = 0.5V_E$ for E_T gives the value of $K_{1/2,E}$ as a function of S and A_T:

$$K_{1/2,E} = A_T/2 + K_1K_2/(K_2 + S) \quad (57a)$$

(*B*) *Partial Random Model.* (*1*) *Initial Velocity.* The conservation equations for the partial random model are eq 1a, 3a, and

$$A_T = A + AS + AE + AES \quad (58a)$$

To obtain the velocity equation for the partial random model, we simply set the parameter K_6 equal to zero in the equations for the fully random model. Thus, we set $K_6 = 0$ in eq 51a to obtain, after simplification of eq 50a (using the equilibrium relation $K_1K_2 = K_3K_4$), the velocity equation:

$$v = 0.5k_{cat}[S/(S + K_2)][R_0 - \mathrm{SQR}(R_0^2 - 4E_TA_T)] \quad (59a)$$

where

$$R_0 = A_T + E_T + K_4(S + K_3)/(S + K_2) \quad (60a)$$

(*2*) *Maximum Velocity.* The V_{max} for this model is obtained by letting S approach infinity in eq 59a and 60a, noting that the ratio terms containing S approach 1:

$$V_{max} = 0.5k_{cat}[H_4 - \mathrm{SQR}(H_4^2 - 4A_TE_T)] \quad (61a)$$

where

$$H_4 = A_T + E_T + K_4$$

(*3*) $K_{m\,app}$. The $K_{m\,app}$ for the partial random model is the root S of the equation $v = 0.5V_{max}$, using the expressions given in eq 59a and 61a. The algebra is complicated, and the re-

sulting equation is basically a quartic in S. However, its root can be expressed as follows:

$$K_{m\,app} = V_9K_2\{H_1 - V_9 - \mathrm{SQR}[(H_1 - V_9)^2 - H_0]\}/H_0 \quad (62a)$$

where

$$H_1 = E_T + A_T + K_1$$

$$H_4 = E_T + A_T + K_4$$

$$V_9 = 0.5[H_4 - \mathrm{SQR}(H_4^2 - 4E_TA_T)]$$

and

$$H_0 = V_9^2 - 2V_9H_4 + 4E_TA_T$$

(*4*) *Enzyme Titrations.* To obtain the maximum velocity for an enzyme titration curve, we take the limit as E_T approaches infinity in eq 59a and 61a. This is more easily accomplished if the term in the brackets in eq 59a is rearranged to form

$$4E_TA_T/[R_0 + \mathrm{SQR}(R_0^2 - 4E_TA_T)]$$

Dividing the numerator and denominator of this term by E_T and then letting E_T go to infinity yield the value $2A_T$. Consequently, we obtain

$$V_E = k_{cat}A_TS/(S + K_2) \quad (63a)$$

Solving the equation $v = 0.5V_E$ for E_T gives the value of $K_{1/2,E}$ as a function of S and A_T:

$$K_{1/2,E} = A_T/2 + K_1(1 + S/K_3)/(1 + S/K_2) \quad (64a)$$

As $S \rightarrow \infty$

$$K_{1/2,E} \rightarrow A_T/2 + K_1K_2/K_3 = A_T/2 + K_4 \quad (65a)$$

and, as $S \rightarrow 0$

$$K_{1/2,E} \rightarrow A_T/2 + K_1 \quad (66a)$$

Equilibrium Version of Conformational Transition Model VII

Initial Velocity. Here we consider a model in which the complexes EA and EA* are in equilibrium: model VII with k_5 replaced by K_5. For this model, the conservation equations are

$$E_T = E + AE + AES + AE^* + AE^*S \quad (67a)$$

$$A_T = A + AE + AES + AE^* + AE^*S \quad (68a)$$

$$S_T \approx S \quad (69a)$$

The fundamental velocity equation is

$$v = k_{cat}AE^*S \quad (70a)$$

The initial velocity equation for this model in terms of total enzyme, activator, and substrate is

$$v = (0.5k_{cat}S/K_3K_2M_1)[R_1 - \mathrm{SQR}(R_1^2 - 4A_TE_T)] \quad (71a)$$

where

$$M_1 = 1 + K_4/K_2K_3 + S(1 + 1/K_3)/K_2$$

and

$$R_1 = E_T + A_T + K_1/M_1$$

Maximum Velocity. The velocity at infinite substrate is given by

$$V_{max} = k_{cat}\min(E_T,A_T)/(1 + 1/K_3) \quad (72a)$$

$K_{m\,app}$. To determine the $K_{m\,app}$, we solve $v = 0.5V_{max}$ by using algebraic manipulations similar to those used in determining the $K_{m\,app}$ for the fully random model. Using the symmetry of the model, it follows that

$$K_{m\,app} = K_2(Z_1 - K_9)/(1 + 1/K_3) \quad (73a)$$

where

$$K_9 = 1 + K_4/K_2K_3$$

$$L_1 = \min(E_T,A_T)$$

$$L_2 = \max(E_T,A_T)$$

$$D_0 = K_9(K_1 + 2L_2K_9)$$

$$D_1 = K_9(L_1 - 3L_2) - K_1$$

$$D_2 = L_2 - L_1/2$$

and

$$Z_1 = [-D_1 + \mathrm{SQR}(D_1^2 - 4D_0D_2)]/2D_2$$

Ratio of $K_{m\,app}$ When $E >> A$ to When $E = A$, the R_{K_m}. If the EA to EA* reaction is truly reversible, then the estimate, K_1^*, of K_1 measured in the absence of substrate (i.e., under true equilibrium conditions) is related to the true constant by

$$K_1 = K_1^*(1 + 1/K_5)$$

From eq 73a, the values of $K_{m\,app}$ as $E \rightarrow \infty$, denoted $K_{m\,app,\infty}$, and when $E_T = A_T = L$, denoted $K_{m\,app,L}$, are

$$K_{m\,app,\infty} = (1 + K_4/K_3K_2)[K_2/(1 + 1/K_3)] \quad (74a)$$

and

$$K_{m\,app,L} = [Z + \mathrm{SQR}(Z^2 - K_9^2)][K_2/(1 + 1/K_3)] \quad (75a)$$

where

$$K_9 = 1 + K_4/K_2K_3 = 1 + 1/K_5$$

and

$$Z = K_9 + K_1/L$$

From eq 74a and 75a, we may determine the ratio of $K_{m\,app,L}$ to $K_{m\,app,\infty}$ (R_{K_m}):

$$R_{K_m} = 1 + K_1^*/L + \mathrm{SQR}[(1 + K_1^*/L)^2 - 1] \quad (76a)$$

Registry No. Factor VIIa, 65312-43-8; factor X, 9001-29-0; factor Xa, 9002-05-5; factor IX, 9001-28-9; factor IXa, 37316-87-3; tissue factor, 9035-58-9.

REFERENCES

Bach, R., Nemerson, Y., & Konigsberg, W. (1981) *J. Biol. Chem. 256*, 8324.

Bach, R., Oberdick, J., & Nemerson, Y. (1984) *Blood 63*, 393.

Bach, R., Gentry, R., & Nemerson, Y. (1986) *Biochemistry* (preceding paper in this issue).

Carson, S. D., Bach, R., & Carson, S. M. (1985) *Blood 66*, 152.

Hultin, M. B., & Nemerson, Y. (1978) *Blood 53*, 928.

Jesty, J., & Nemerson, Y. (1974) *J. Biol. Chem. 249*, 509.

Jesty, J., & Nemerson, Y. (1976) *Methods Enzymol. 45*, 95.

Kalousek, F., Konigsberg, W., & Nemerson, Y. (1975) *FEBS Lett. 50*, 382.

Kettner, C., & Shaw, E. (1981) *Thromb. Res. 22*, 645.

Laemmli, U. K. (1970) *Nature (London) 227*, 680.

Miletich, J. P., Jackson, C. M., & Majerus, P. W. (1978) *J. Biol. Chem. 253*, 6908.

Milstone, J. H., Oulinoff, N., Saxton, T. F., & Milstone, V. K. (1971) *Yale J. Biol. Med. 43*, 223.

Mimms, L. T., Zampighi, G., Nozaki, Y., Tanford, C., & Reynolds, J. A. (1981) *Biochemistry 20*, 833.

Morrison-Silverberg, S. A., & Jesty, J. (1981) *J. Biol. Chem. 256*, 1625.
Nemerson, Y., & Clyne, L. P. (1974) *J. Lab. Clin. Med. 83*, 301.
Nesheim, M. F., Taswell, J. B., & Mann, K. G. (1979) *J. Biol. Chem. 54*, 10952.
Nesheim, M. F., Tracy, R. P., & Mann, K. G. (1984) *J. Biol. Chem. 259*, 1447.
Pusey, M. L., & Nelsestuen, G. L. (1983) *Biochem. Biophys. Res. Commun. 114*, 526.
Radcliffe, R. D., & Nemerson, Y. (1975) *J. Biol. Chem. 250*, 388.
Radcliffe, R. D., & Nemerson, Y. (1976) *J. Biol. Chem. 251*, 4797.
Repke, D., MacLean, D. E., & Nemerson, Y. (1981) *Fed. Proc., Fed. Am. Soc. Exp. Biol. 40*, 1587.
Reynolds, J. A., Nozaki, Y., & Tanford, C. (1983) *Anal. Biochem. 130*, 471.
Silverberg, S. A., Nemerson, Y., & Zur, M. (1977) *J. Biol. Chem. 252*, 8481.
van de Waart, P., Bruls, H., Hemker, H. C., & Lindhout, T. (1983) *Biochemistry 22*, 2427.
van Rijn, J. L. M. L., Govers-Riemslag, J. W. P., Zwaal, R. F. A., & Rosing, J. (1984) *Biochemistry 23*, 4557.
Zur, M., & Nemerson, Y. (1978) *J. Biol. Chem. 253*, 2203.
Zur, M., & Nemerson, Y. (1982) *Methods Enzymol. 80*, 237.
Zur, M., Radcliffe, R. D., Oberdick, J., & Nemerson, Y. (1982) *J. Biol. Chem. 257*, 5623.

Interaction of Heparin with Plasminogen Activators and Plasminogen: Effects on the Activation of Plasminogen†

Patricia Andrade-Gordon and Sidney Strickland*
Department of Pharmacological Sciences, State University of New York at Stony Brook, Stony Brook, New York 11794-8651
Received November 8, 1985; Revised Manuscript Received April 23, 1986

ABSTRACT: The amidolytic plasmin activity of a mixture of tissue plasminogen activator (tPA) and plasminogen is enhanced by heparin at therapeutic concentrations. Heparin also increases the activity in mixtures of urokinase-type plasminogen activator (uPA) and plasminogen but has no effect on streptokinase or plasmin. Direct analyses of plasminogen activation by polyacrylamide gel electrophoresis demonstrate that heparin increases the activation of plasminogen by both tPA and uPA. Binding studies show that heparin binds to various components of the fibrinolytic system, with tight binding demonstrable with tPA, uPA, and Lys-plasminogen. The stimulation of tPA activity by fibrin, however, is diminished by heparin. The ability of heparin to promote plasmin generation is destroyed by incubation of the heparin with heparinase, whereas incubation with chondroitinase ABC or AC has no effect. Also, stimulation of plasmin formation is not observed with dextran sulfate or chondroitin sulfate A, B, or C. Analyses of heparin fractions after separation on columns of antithrombin III–Sepharose suggest that both the high-affinity and the low-affinity fractions, which have dramatically different anticoagulant activity, have similar activity toward the fibrinolytic components.

Heparin, a complex glycosaminoglycan isolated from a variety of natural sources, is a valuable anticoagulant due to the rapidity of its action. In contrast to the oral anticoagulants that take hours to exhibit their activity, heparin is almost immediately effective upon intravenous injection. This action is primarily due to a complex that is formed in blood between heparin and antithrombin III (AT-III).[1] Whereas AT-III is a slow inhibitor of thrombin and other clotting proteases, the heparin–AT-III complex can very rapidly inhibit these enzymes (Rosenberg & Damus, 1973), thereby inhibiting clot formation. Interestingly, after irreversible inhibition of thrombin by the heparin–AT-III complex, heparin can be released to bind to another molecule of AT-III and facilitate its inhibition of another thrombin molecule (Jordan et al., 1979). Thus, heparin acts catalytically to disrupt the final stages of the blood clotting cascade.

Although commercial heparin is a complex mixture of glycosaminoglycans, the molecular aspects that govern its interaction with AT-III are becoming clearer due to fractionation of the commercial preparations on the basis of binding to AT-III and chemical analysis of the fractions that bind (Lam et al., 1976; Hook et al., 1976; Andersson et al., 1976). It appears that a pentasaccharide sequence that contains a unique 3-sulfate is necessary for tight binding to AT-III (Thunberg et al., 1982; Choay et al., 1983).

Heparin therapy, in addition to the desired effect of preventing clot formation, has in many cases undesirable consequences. The most pronounced adverse reactions are hemorrhage and thrombocytopenia (O'Reilly, 1985), the latter of which may be a consequence of heparin-induced platelet aggregation via anti-heparin antibodies (Cines et al., 1980).

Although the binding of heparin to AT-III may explain many of its anticoagulant properties, it is known that heparin also binds to other proteins that could possible influence its effects in vivo. These proteins include, for example, factor IX

†Supported by grants from the National Institutes of Health (HD 17875), American Cancer Society (CD 48), American Heart Association (84 1242), and New York Science and Technology Foundation (X043). S.S. is an Established Investigator of the American Heart Association.

[1] Abbreviations: AT-III, antithrombin III; tPA, tissue-type plasminogen activator; uPA, urokinase-type plasminogen activator; SK, streptokinase; SDS–PAGE, sodium dodecyl sulfate–polyacrylamide gel electrophoresis; H-D-Val-Leu-Lys-pNA, D-valyl-L-leucyl-L-lysine-*p*-nitroanilide; H-D-HHT-Ala-Arg-pNA·2OAc, D-hexahydrotyrosyl-L-alanyl-L-arginine-*p*-nitroanilide diacetate salt; Tris-HCl, tris(hydroxymethyl)-aminomethane hydrochloride; EDTA, ethylenediaminetetraacetic acid.

0006-2960/86/0425-4033$01.50/0